

The effect of the warping deformation on the structural behaviour of thin-walled open section shear walls



Alberto Carpinteri^a, Giuseppe Lacidogna^{a,*}, Bartolomeo Montrucchio^b, Sandro Cammarano^a

^a Department of Structural, Geotechnical and Building Engineering, Politecnico di Torino, Corso Duca degli Abruzzi 24, 10129 Torino, Italy

^b Department of Control and Computer Engineering, Politecnico di Torino, Corso Duca degli Abruzzi 24, 10129 Torino, Italy

ARTICLE INFO

Article history:

Received 20 January 2014

Received in revised form

8 July 2014

Accepted 8 July 2014

Keywords:

Vlasov's theory

Warping deformation

Tall buildings

External load distribution

Bimoment action

Optical analysis

ABSTRACT

Thin-walled open section beams are carefully analysed by Vlasov's theory of the sectorial areas. It allows to take into account their peculiar warping deformation which appears in the presence of torsional actions. This behaviour determines a further stress state along the axis of the element which is rarely considered in structural analyses. The aim of the present paper is the evaluation of the warping deformation of thin-walled open section beams subjected to torsion. Firstly, the analytical theory proposed by Vlasov is verified through an experimental test on a steel specimen defined by a U profile. Specific analyses are performed with the aim of a sophisticated optical device in order to assess the transverse distortion of the section. Then, the results obtained experimentally and confirmed by a Finite Element (FE) programme permit to validate a computer programme based on the analytical theory and devised to study the structural behaviour of high-rise buildings stiffened by thin-walled open section shear walls. In order to evaluate the effectiveness of the programme, an example which highlights the benefits provided by the present method compared to FE programme is carried out.

© 2014 Elsevier Ltd. All rights reserved.

1. Introduction

In the design of high-rise building the identification of an adequate resistant system able to absorb the horizontal actions coming from earthquakes and wind is a crucial point of the design process. The structural schemes usually employed to stiffen horizontally a building are several and the choice of one of them is certainly function of the characteristics of the structure, in particular the total height. The evolution of the construction techniques as well as the limits imposed by legislation in terms of displacements have determined a clear distinction between all the possible structural solutions. Nevertheless, the choice of a specific solution can also depend on the functional needs required by the building occupants. In particular, the presence of systems which allow a rapid usability of the floor spaces may address the engineer's judgment. In this direction, indeed, thin-walled open sections bracings prove to be doubly convenient: from the usability point of view, they are able to house the elevator shaft and the stairwell, whereas, from the structural point of view, they

contribute to the horizontal stiffness of the resistant skeleton and, therefore, to the stability of the construction.

It is well-known that such elements, if subjected to torsional actions, show a peculiar deformation, known as warping deformation, which is described by the distortion of the section out of its own plane. This phenomenon is caused by a particular internal action, called bimoment, which determines a further stress state having an intensity comparable to that coming from flexural actions.

Therefore, it is clear that an accurate design of these elements cannot disregard their unusual torsional deformation, especially in those situations in which their resistant contribution proves to be determinant for the lateral stability of the construction.

The early analytical formulations focused on the structural behaviour of thin-walled open section profiles were proposed, almost at the same time, by Vlasov [1–3] and Timoshenko [4]. In particular, the former examined in depth these elements, giving rise to a comprehensive theory of which the well-known Saint Venant theory proved to be a very special case. Many works related to this topic followed trying to extend this original formulation, which, however, remains a milestone in the study of structural mechanics.

To authors' best knowledge, papers regarding experimental tests for the assessment of the warping deformation of thin-walled open section beams subjected to torsional actions are almost absent in literature.

* Corresponding author. Tel.: +39 110904871; fax: +39 110904999.

E-mail addresses: alberto.carpinteri@polito.it (A. Carpinteri), giuseppe.lacidogna@polito.it (G. Lacidogna), bartolomeo.montrucchio@polito.it (B. Montrucchio), sandro.cammarano@polito.it (S. Cammarano).

and the sectorial products of inertia $I_{\omega x}$ and $I_{\omega y}$ vanish as well. Therefore, the system (1) is reduced to

$$\begin{aligned} EA\zeta'' &= q_z \\ EI_y \xi^{IV} &= q_x \\ EI_x \eta^{IV} &= q_y \\ EI_\omega \vartheta^{IV} - GJ_t \vartheta'' &= m \end{aligned} \tag{2}$$

The equations, initially coupled each other through the variables ξ, η, ζ and ϑ , are now independent. In Eq. (2d) the term which refers to de Saint Venant theory, that is proportional to the torsional stiffness GJ_t , is, for now, disregarded. Its contribution will be added later, in the final expression which defines the stiffness matrix of the element.

If the system of external forces is only represented by transverse actions, Eq. (2a) can be neglected. The remaining equations can be organized in a matrix form through the following vectors of the displacements δ and the actions q :

$$\delta = \begin{Bmatrix} \xi \\ \eta \\ \vartheta \end{Bmatrix} \quad q = \begin{Bmatrix} q_x \\ q_y \\ m \end{Bmatrix} \tag{3}$$

$$EI\delta^{IV} = q \tag{4}$$

in which \mathbf{I} is a diagonal 3×3 matrix whose diagonal coefficients are expressed by I_y, I_x and I_ω , being all the other elements equal to zero.

Since \mathbf{I} is symmetrical and positive definite until the geometry of the section is such that the corresponding sectorial moment of inertia I_ω is different from zero, it is possible to invert the expression (4) in order to highlight the vector of displacements δ .

$$\delta^{IV} = \mathbf{I}^{-1}q/E \tag{5}$$

If the actions are not represented by forces distributed along the beam, but are defined by concentrated loads in correspondence to N specific sections (Fig. 2a), Eq. (5) remains valid in each field circumscribed by these sections and shows the following form:

$$\delta^{IV} = \mathbf{I}^{-1}0/E \tag{6}$$

or, exploiting the concentrated actions,

$$\delta''' = -\mathbf{I}^{-1}F/E \tag{7}$$

where the vector F is directly connected to the vector q as follows:

$$q = -\frac{\partial}{\partial z}F = -\frac{\partial}{\partial z} \begin{Bmatrix} F_x \\ F_y \\ M_z \end{Bmatrix} \tag{8}$$

The transverse displacements ξ, η and ϑ are acquired integrating Eq. (6) in each field where the expression is defined and introducing the adequate boundary conditions. Such conditions are subdivided in continuity and global conditions.

The continuity conditions for the j -th section ($j=2, \dots, N$) are:

$$\begin{aligned} \delta(j)_{j-1/j} &= \delta(j)_{j/j+1} \\ \delta'(j)_{j-1/j} &= \delta'(j)_{j/j+1} \\ \delta''(j)_{j-1/j} &= \delta''(j)_{j/j+1} \\ EI\delta'''(j)_{j-1/j} &= EI\delta'''(j)_{j/j+1} + F(j) \end{aligned} \tag{9}$$

in which the first two are kinematic, whereas the last are equilibrium conditions (Fig. 2b).

If the beam is constrained as a cantilever beam, the global conditions for the free edge ($j=1$) are given by equilibrium conditions:

$$\begin{aligned} \delta'(1) &= 0 \\ \delta'''(1) &= -\mathbf{I}^{-1}F(1)/E \end{aligned} \tag{10}$$

whereas, for the opposite edge ($j=N+1$), kinematic conditions are considered.

$$\begin{aligned} \delta(N+1) &= 0 \\ \delta'(N+1) &= 0 \end{aligned} \tag{11}$$

For the sake of simplicity, the transverse displacements of the sections are reported in a single $3N$ -vector δ , in which the translations along the X axis, then those along the Y axis and finally the rotations are posed. Similarly a global $3N$ -vector F containing N shear forces F_x, N shear forces F_y and, finally, N torque moments M_z is assembled.

By means of the procedure of integration previously mentioned, it is possible to obtain a relationship between δ and F through the compliance matrix \mathbf{C} or its inverse, the stiffness matrix \mathbf{k} .

$$\underline{\delta} = \mathbf{C}\underline{F} = \mathbf{k}^{-1}\underline{F} \tag{12}$$

Finally the torsional contribution coming from de Saint Venant theory, which is proportional to the torsional inertia J_t , is added to the torsional component of the calculated stiffness matrix.

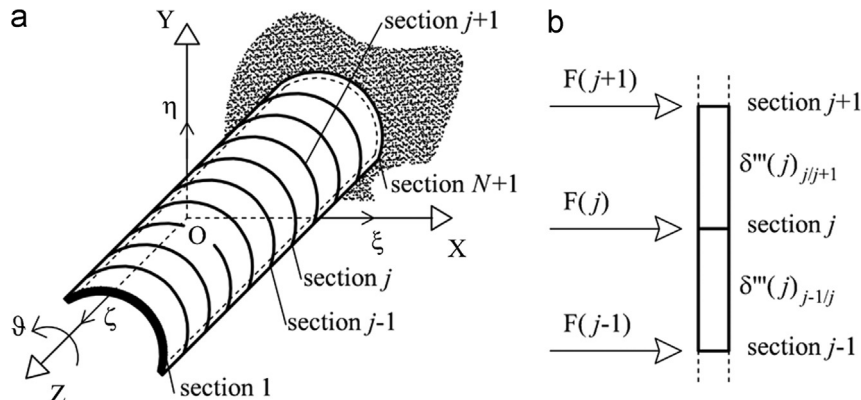


Fig. 2. Thin-walled open section beam subjected to concentrated transverse actions applied to specific sections (a); scheme for the continuity conditions between different sections (b).

Once the external actions are known, by means of Eq. (12), it is possible to obtain the displacements of the corresponding sections in terms of ξ , η and θ . Then, deriving the latter with respect to the coordinate z and exploiting Eq. (13), the axial displacements which define the warping of the section are simply deduced, according to the theory of the sectorial areas.

$$w(z, s) = -\vartheta'(z)\omega \tag{13}$$

2.2. Experimental investigation on the warping deformation of thin-walled open section beams

Specific experimental investigations for the evaluation of the effective out-of-plane distortion of thin-walled open section beams subjected to torsional actions are almost absent in the literature of the past fifty years. Therefore, the contribution described below proves to be particularly innovative for the structural analysis of these thin-walled profiles.

The evaluation of the warping deformation is performed by means of an experimental test on a 1.6 m long steel beam, constrained as an horizontal cantilever. The cross-section is defined by a thin-walled U profile (Fig. 3).

The rigid constraint is realized at one of the edges of the beam by means of welding on a steel plate, which is bolted to a fixed system (Fig. 3, plate A).

On the upper flange, at distance of 0.16 m each other, some little beams, having L-shaped section and conveniently altered for the application of the transverse actions, are welded. The geometrical dimensions of the structural components are reported in Fig. 4.

The applied loads are represented by masses, each of 3.08 kg, located at 0.23 m far from the shear centre of the U-shaped section. In this way, at the same time, shear forces and anticlockwise torsional moments are produced (Fig. 5).

The system for detecting the axial displacements defining the warping of the section is constituted by three main components. The first is a little steel frame which is connected, through bolts, to



Fig. 5. Application of the external concentrated loads.

the L-shaped section beam posed at the free edge of the examined U-shaped section beam.

The second is a laser, rigidly connected to the steel frame, whose ray is directed to the free edge of the bottom flange of the U-shaped profile (Fig. 6a).

The last is a spherical mirror, characterized by specific geometrical properties adequate for precision measurements (Table 1), which is placed where the ray meets the bottom flange of the main beam. According to this configuration, the ray of the laser is reflected on the inner side of the upper flange of the U-shaped section beam, where a ruler is pasted (Figs. 6b and 7).

Because of the concentrated torsional moments, the section twists around its shear centre, undergoing, at the same time, a distortion out of its own plane. This deformation can be expressed by the system of axial displacements of the points constituting the section, once the pure flexural deformations are removed.

Experimentally, it may be evaluated considering the relative axial displacement of two symmetrical points of the section: in particular, as regard the performed test, the relative displacement of the points corresponding to the laser (A→A') and the mirror (B→B') is measured (Fig. 8).

Exploiting the geometrical properties of the mirror, as a consequence of the displacement s of the incident ray, it is possible to detect, on the upper flange of the U-shaped section, the displacement s' related to the corresponding reflected ray. Because of the curvature of the mirror, the term s' represents an amplification of s and, therefore, its measurement becomes much easier (Fig. 9).

In this case, the geometrical characteristics of the mirror are such that the amplification factor, that is the ratio between s' and s , is about 12.

The experimental analysis has been conducted varying the loading condition: in a first phase the L-shaped section beams have been loaded, each with one mass of 3.08 kg, progressively from $z=0.48$ m to $z=1.44$ m, being $z=0$ m the constrained edge of the beam; then, the unloading process has been performed according to the same order (Fig. 10).

In Fig. 11 the experimental results, which describe the amplified displacement s' related to the loading phase, are reported. It is evident that the use of the optical device facilitates the detection of displacements which are, otherwise, invisible to the naked eye.

The same structure has, finally, been modelled in a Finite Element programme in order to verify the effectiveness of the analytical method in the individuation of the structural behaviour of thin-walled open section beams. In this case, the steel U-shaped section beam has been modelled by means of thin shell elements. In Table 2 the numerical comparison between the analytical and the FE method is shown and a good convergence can be acknowledged, since the main difference is about 4%.

Similarly, the same correspondence can be noticed comparing the numerical results with experimental ones: in Fig. 12 normalized values of the axial displacement s are reported taking into

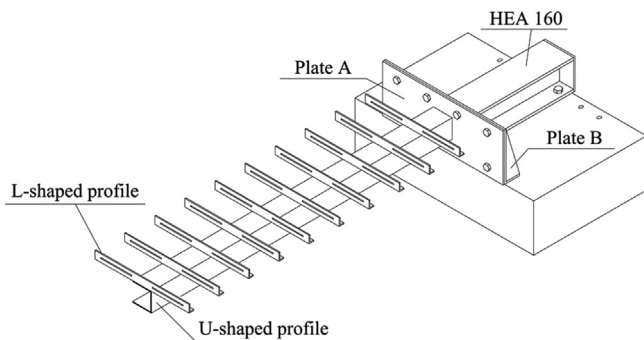


Fig. 3. Scheme of the test on a thin-walled U-shaped section steel beam.

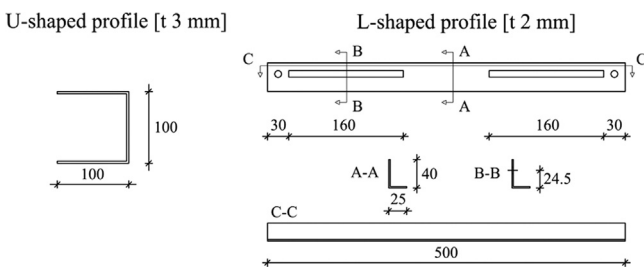


Fig. 4. Geometric properties of the thin-walled steel profiles.

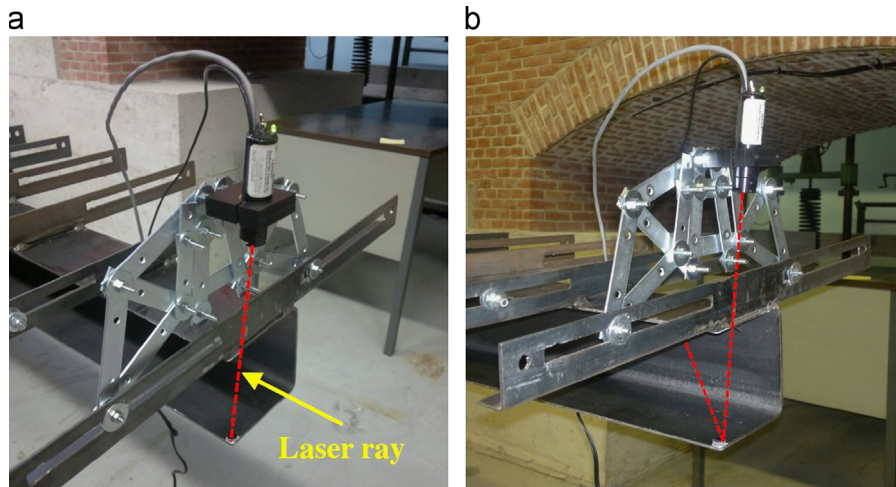


Fig. 6. Picture of the little steel frame, applied to the extreme L-shaped profile, to which the laser is connected (a); scheme of the reflection of the laser (b).

Table 1
Geometrical and focal properties of the spherical mirror.

Diameter [mm]	10.00	Surface quality	60–40
Effective focal length EFL [mm]	10.00	Surface accuracy (λ)	1/4
Radius R [mm]	20.00	Diameter tolerance [mm]	+0/–0.30
Edge thickness ET [mm]	3.63	Focal length tolerance [%]	± 2
Centre thickness CT [mm]	3.00	Centre thickness tolerance [mm]	± 0.30

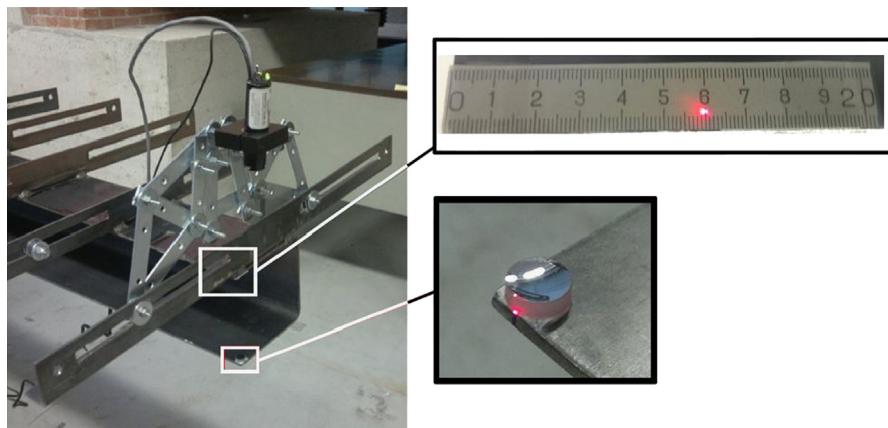


Fig. 7. Location of the optical device and the ruler which allows the measurement of the warping of the section.

account every single loading condition, during both the loading and unloading process.

Since Vlasov's theory proves to reach enough accuracy, until the material is linear elastic, the proposed analytical formulation can be easily extended to consider beams with greater dimensions, as the case of thin-walled open section bracings which are usually employed to stiffen horizontally tall buildings.

3. Structural analysis of high-rise buildings

The analytical formulation introduced in the previous section can be employed for the evaluation of the structural behaviour of high-rise buildings stiffened by thin-walled open section shear walls. The previous analytical method can be directly included in the three-dimensional formulation proposed by Carpinteri et al. [10,11], which allows to consider various vertical bracings, randomly arranged in the building plan.

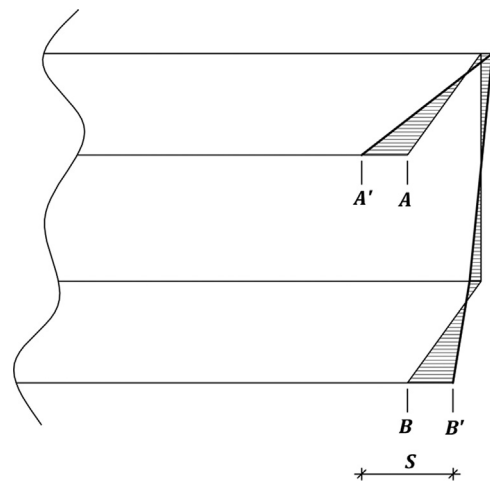


Fig. 8. Relative displacement s between the laser ($A \rightarrow A'$) and the mirror ($B \rightarrow B'$).

The implementation of the latter formulation, compared to Finite Element methods which are usually employed in the design of these complex structures, provides some advantages, especially in the preliminary phases when several structural configurations are examined in depth. The reduction of the modelling time and the clearness of the approach represent the first achieved benefits of the method. The former fulfills the need of carrying out numerous analyses aimed to identify the best structural solution for specific loading cases; the latter, derived from precise

hypotheses, allows to obtain information regarding the main parameters on which the structural behaviour of these constructions depends. Further advantages can be underlined: among all, the capability of the method to distinctly describe the external load distribution between different types of vertical bracings, which constitute the structural skeleton of the building. Finally, aimed to perform a preliminary design, for each structural element, the trend of the main internal actions, also including the bimoment action related to the case of thin-walled open section members, can be evaluated.

In order to highlight the aforementioned capabilities of the three-dimensional formulation, a numerical example regarding a tall building loaded by transverse static actions is now carried out. In this specific case, the resistant core of the whole structure is composed by three thin-walled open section members, having different cross-sections.

The building is 200 m high and characterized by a storey height of 5 m. The structural material of the bracings is concrete whose mechanical properties are given by Young's modulus and Poisson's ratio equal to 3×10^4 MPa and 0.18 respectively. The effects related to creep and shrinkage are not taken into account in the analysis.

The dimensions and the geometrical properties of the cantilevers are shown respectively in Fig. 13 and in Table 3.

The static loading condition is represented by concentrated resultant forces applied to the floors in correspondence to the

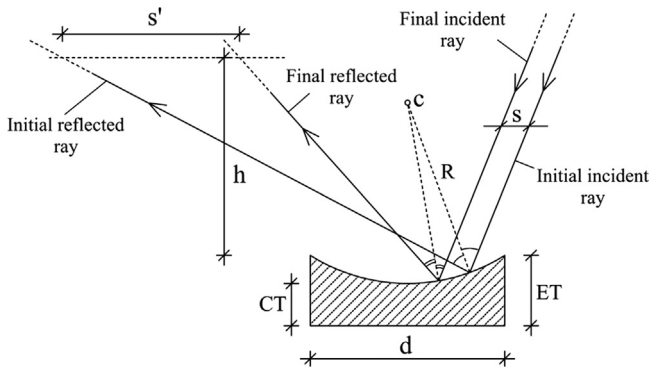


Fig. 9. Amplification of s due to the geometric characteristics of the spherical mirror.

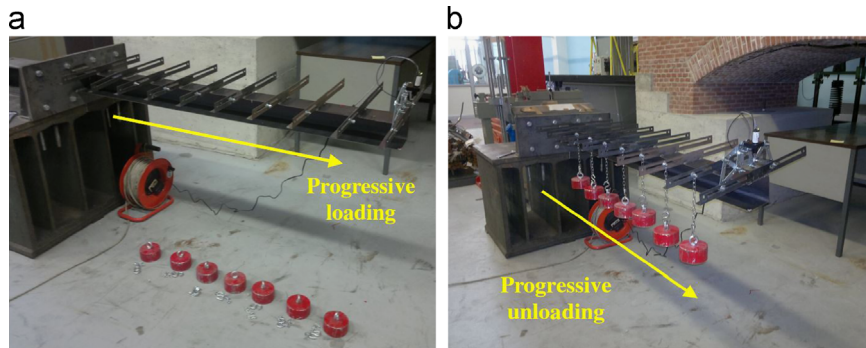


Fig. 10. Different loading conditions: (a) loading and (b) unloading phase.

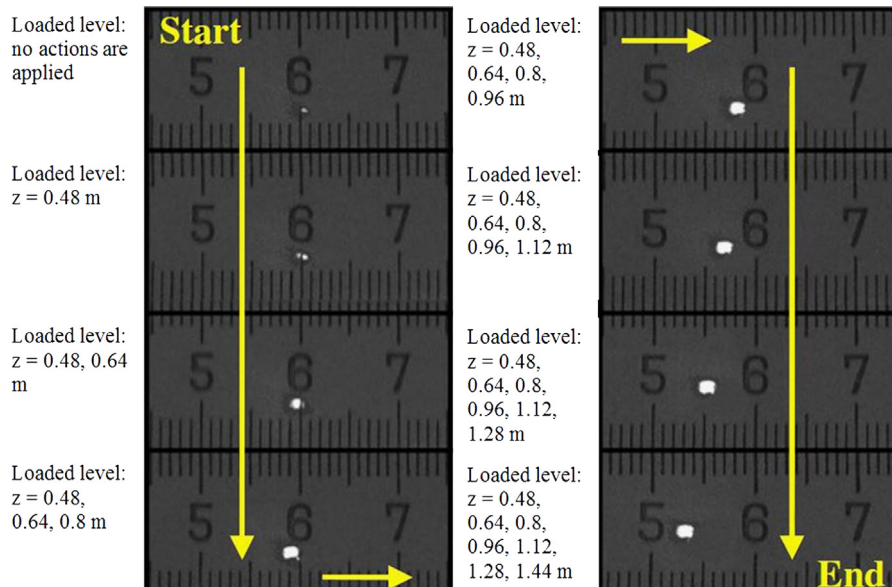


Fig. 11. Measurement of the displacement s' during the loading phase: the white dots represent the consecutive positions of the reflected ray on the ruler.

Table 2
Comparison between analytical and FE method.

Type of process		Loading				Unloading			
Level N.	z [m]	Loaded level	s [mm]		Err. [%]	Loaded level	s [mm]		Err. [%]
			Analytic.	FEM			Analytic.	FEM	
1	0.48	1	7.61 E-03	7.56 E-03	0.61	1–7	2.52 E-01	2.46 E-01	2.58
2	0.64	1, 2	2.13 E-02	2.10 E-02	1.23	2–7	2.44 E-01	2.38 E-01	2.64
3	0.80	1–3	4.29 E-02	4.22 E-02	1.56	3–7	2.31 E-01	2.25 E-01	2.71
4	0.96	1–4	7.44 E-02	7.32 E-02	1.74	4–7	2.09 E-01	2.03 E-01	2.79
5	1.12	1–5	1.18 E-01	1.16 E-01	1.86	5–7	1.77 E-01	1.72 E-01	2.94
6	1.28	1–6	1.76 E-01	1.73 E-01	2.00	6, 7	1.34 E-01	1.30 E-01	3.23
7	1.44	1–7	2.52 E-01	2.46 E-01	2.58	7	7.54 E-02	7.26 E-02	3.95

Error [%]=(Analytical–FEM)/FEM × 100.

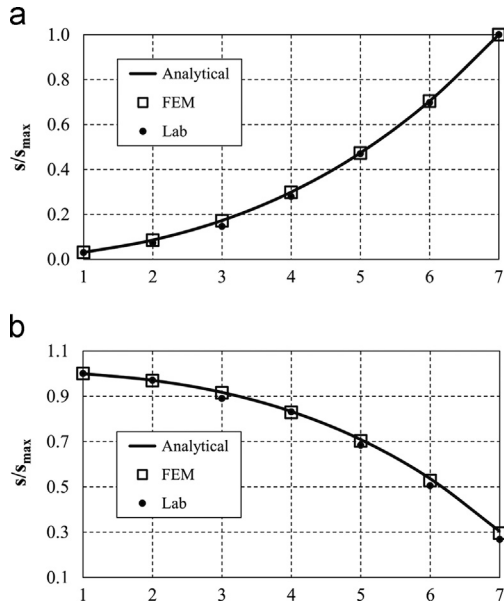


Fig. 12. Comparison of the results in terms of normalized values of the axial displacement *s*, during the (a) loading and (b) unloading process.

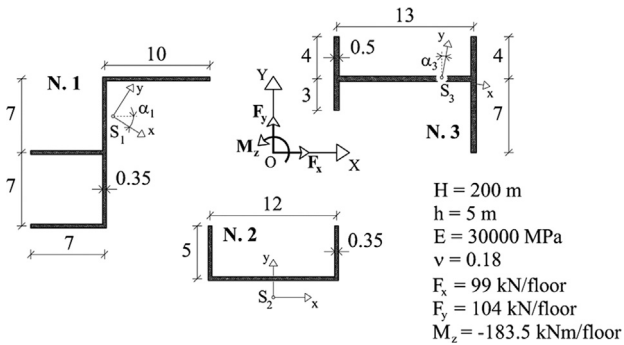


Fig. 13. Internal core system of a tall building constituted by thin-walled open section shear walls (measures in metres).

origin of the global coordinate system XYZ (Fig. 13). In particular, along the X direction a resultant force of 99 kN for each floor is considered, whereas in the Y direction it becomes equal to 104 kN. In this specific loading case a clockwise torsional moment of 183.5 kNm is taken into account.

This structural scheme is modelled through both the present method and a computer programme implementing the FE method.

Table 3
Geometrical properties of the shear walls.

Element N.	1	2	3
I_x [m ⁴]	483.45	19.22	71.18
I_y [m ⁴]	80.76	176.40	469.99
I_w [m ⁶]	3611.67	487.50	1997.06
J_t [m ⁴]	0.54	0.31	1.29
X_s [m]	-15.21	0.00	16.45
Y_s [m]	3.43	-13.79	6.97
α [°]	-32.45	0.00	-8.69

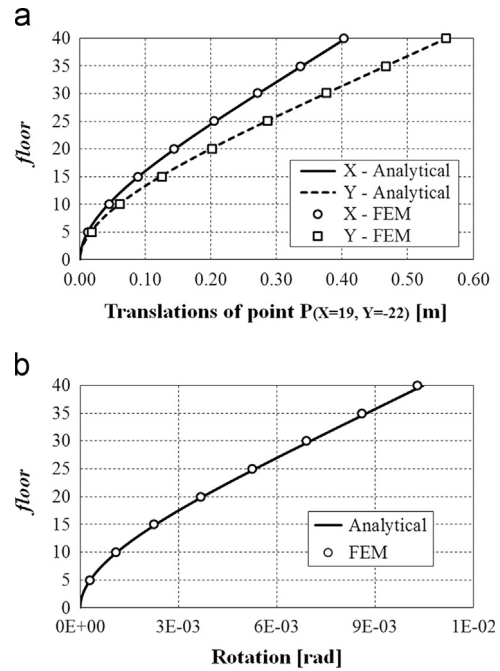


Fig. 14. Comparison between the analytical and FE method in terms of displacements of the building.

The results with which the comparison is performed are expressed in terms of displacements, in particular translations and rotations of the floors according to the global coordinate system XYZ. The corresponding curves are reported in Fig. 14.

It is self-evident the outstanding convergence of the methods, which confirms the usability of the analytical formulation at least in the first phases of the design process.

Further structural information achievable from the proposed method are reported in Figs. 15 and 16. In the first case the

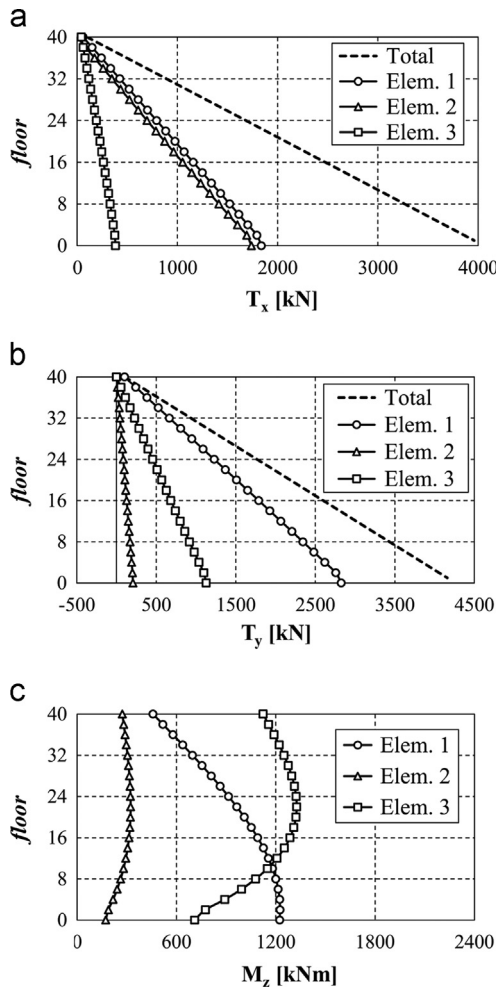


Fig. 15. External load distribution between the components of the core system in terms of shears in the (a) X and (b) Y direction and (c) torque.

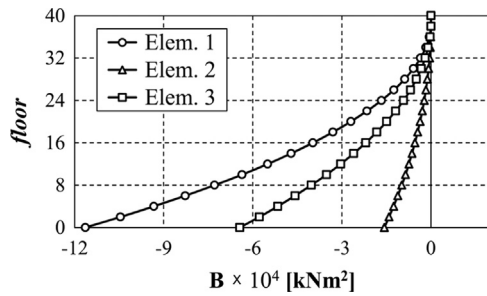


Fig. 16. Bimoment action in the shear walls constituting the core system.

Element N.	1	2	3
M_x [kNm]	-350313.09	-20827.37	-116807.38
M_y [kNm]	2776.34	171628.43	26628.93
B [kNm ²]	-116436.02	-15716.44	-64382.83

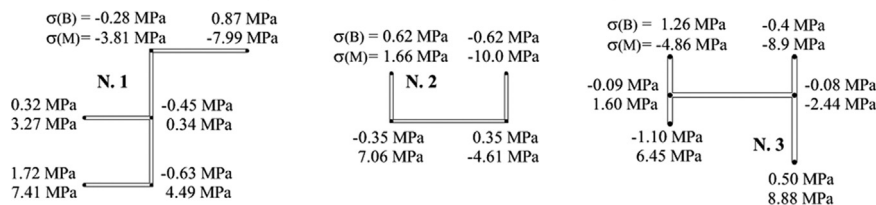


Fig. 17. Comparison of the stress state due to bending and warping of the walls.

distribution of the shears T_x , T_y and the torque M_z between the bracings is pointed out.

This description can represent an outstanding support in the design process since it facilitates the individuation of the most stressed element as well as a good comprehension of the force flow within the structural skeleton of the construction. In addition, unlike FE simulations, as regard thin-walled open section elements, also the bimoment action, which is known as the cause of the warping of this type of section, can be evaluated. The main effect of this uncommon internal action is the development of an additional state of stresses defined by normal and tangential components. Their intensity can be, in some cases, comparable to the one derived from pure flexural behaviour. Therefore, since the latter can affect the structural behaviour of the entire building, at least an approximate evaluation of the bimoment action during the preliminary design has to be carried out.

In Fig. 16 the curves of bimoment corresponding to each shear wall constituting the internal core of the construction are shown, whereas in Fig. 17 information regarding the additional stress state in terms of normal components are reported. In the latter figure, a comparison with the stress state caused by the pure bending behaviour is highlighted and it can be seen that, in some cases, the bimoment action determines an increase in tension of about 20–30%.

4. Conclusions

The present paper is focused on the analysis of the warping deformation of thin-walled open section beams, subjected to torsional actions. For this purpose, an experimental test regarding a thin-walled beam having U profile loaded by shears and torsional forces has been performed. With the aim of an adequate optical device the out-of-plane distortion of the section has been identified. The results obtained by the experimental test compared to those calculated by a FE programme and by the proposed analytical method have shown a good convergence. Therefore, the analytical formulation can be also considered as a suitable tool for the structural analysis of high-rise structures stiffened by thin-walled open section bracings. By means of it, some advantages compared to FE methods can be achieved: firstly the reduction of modelling time and the clearness of the procedure employed by the approach as well as the capability of providing information regarding the main parameters which describe the structural behaviour of these complex constructions. Furthermore, the external load distribution between different types of bracings and the trend of the main internal actions acting in each structural element can be clearly derived. Finally, as regard the case of thin-walled open section members, the bimoment action which is the cause of the warping deformation of open sections, can be evaluated to perform a thorough preliminary design.

Acknowledgements

The financial support provided by the Ministry of University and Scientific Research (MIUR) for the Ph.D. scholarship “Tall buildings constructed with advanced materials: a global approach for the analysis under static and dynamic loads”, is gratefully acknowledged.

References

- [1] Vlasov VZ. A new method of designing thin-walled prismatic shells for combined action of axial force, bending and torsion. *Vestnik VIA RSKA* 1936;20 [in Russian].
- [2] Vlasov VZ. Structural mechanics of thin-walled spatial systems. Moscow: Gosstroizdat; 1949 [in Russian].
- [3] Vlasov VZ. Thin-walled elastic beams. Washington: US Science Foundation; 1961.
- [4] Timoshenko S. Theory of bending, torsion and buckling of thin-walled members of open cross section. *J Frankl Inst* 1945;239:201–361.
- [5] Ambrosini D. On free vibration of non-symmetrical thin-walled beams. *Thin-Walled Struct* 2009;47:629–36.
- [6] Ambrosini D. Experimental validation of free vibrations from non-symmetrical thin walled beams. *Eng Struct* 2010;32:1324–32.
- [7] Klausbruckner MJ, Pryputniewicz RJ. Theoretical and experimental study of coupled vibrations of channel beams. *J Sound Vib* 1995;183:239–52.
- [8] Rendek S, Baláz I. Distortion of thin-walled beams. *Thin-Walled Struct* 2004;42:255–77.
- [9] Dufort L, Grédiac M, Surrel Y. Experimental evidence of the cross-section warping in short composite beams under three point bending. *Compos Struct* 2001;51:37–47.
- [10] Carpinteri A, Carpinteri An. Lateral loading distribution between the elements of a three-dimensional civil structure. *Comput Struct* 1985;21:563–80.
- [11] Carpinteri A, Lacidogna G, Puzzi S. A global approach for three dimensional analysis of tall buildings. *Struct Des Tall Spec Build* 2010;19:518–36.
- [12] Carpinteri A, Corrado M, Lacidogna G, Cammarano S. Lateral load effects on tall shear wall structures of different height. *Struct Eng Mech* 2012;41:313–37.